

Electronic Supporting Information for

Poly(phenylene-ethynylene-*alt*-tetraphenylethene) Copolymers:

Aggregation Enhanced Emission, Induced Circular Dichromism, Tunable
Surface Wettability and Sensitive Explosive Detection

Xiao Wang^a, Wenjie Wang^a, Yanmei Wang^a, Jing Zhi Sun^{*a} and Ben Zhong Tang ^{*abc}

a MOE Key Laboratory of Macromolecular Synthesis and Functionalization, Department of
Polymer Science and Engineering, Zhejiang University, Hangzhou 310027, China. E-mail:
sunjz@zju.edu.cn.

b Guangdong Innovative Research Team, State Key Laboratory of Luminescent Materials and
Devices, South China University of Technology, Guangzhou 510640, China

c Department of Chemistry, Institute for Advanced Study, Institute of Molecular Functional
Materials, and State Key Laboratory of Molecular Neuroscience, The Hong Kong University of
Science and Technology, Clear Water Bay, Kowloon, Hong Kong, China. E-mail: tangbenz@ust.hk

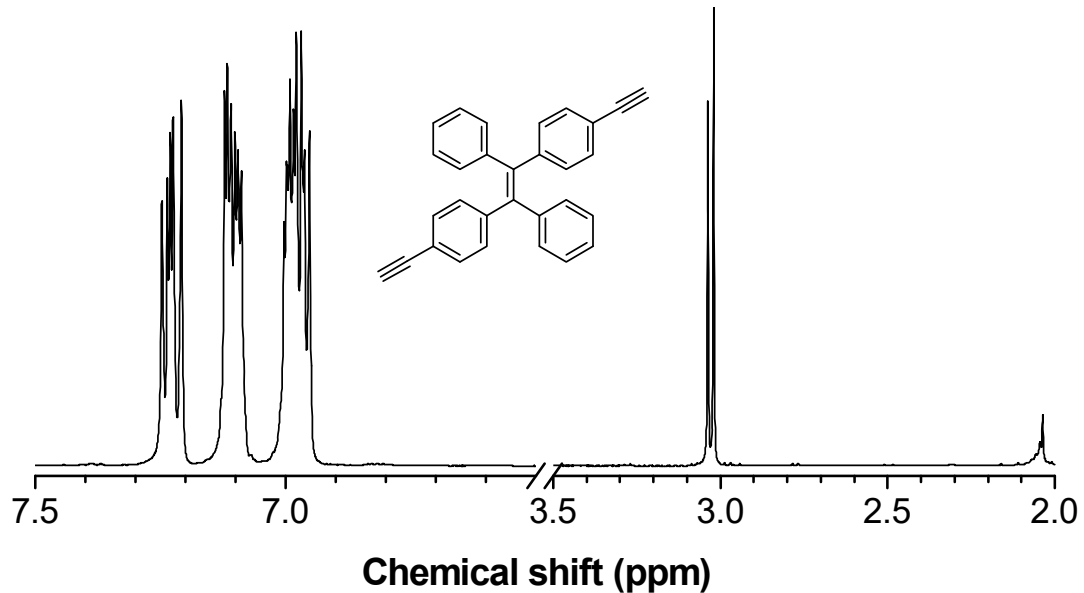


Figure S1. ^1H NMR spectrum of **BETPE** in CDCl_3 .

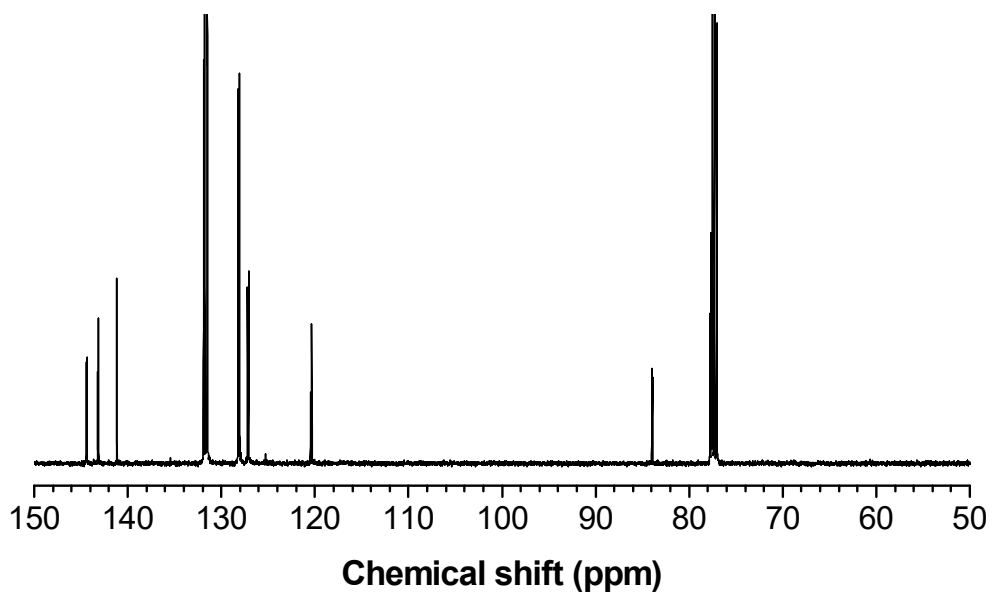


Figure S2. ^{13}C NMR spectrum of **BETPE** in CDCl_3 .

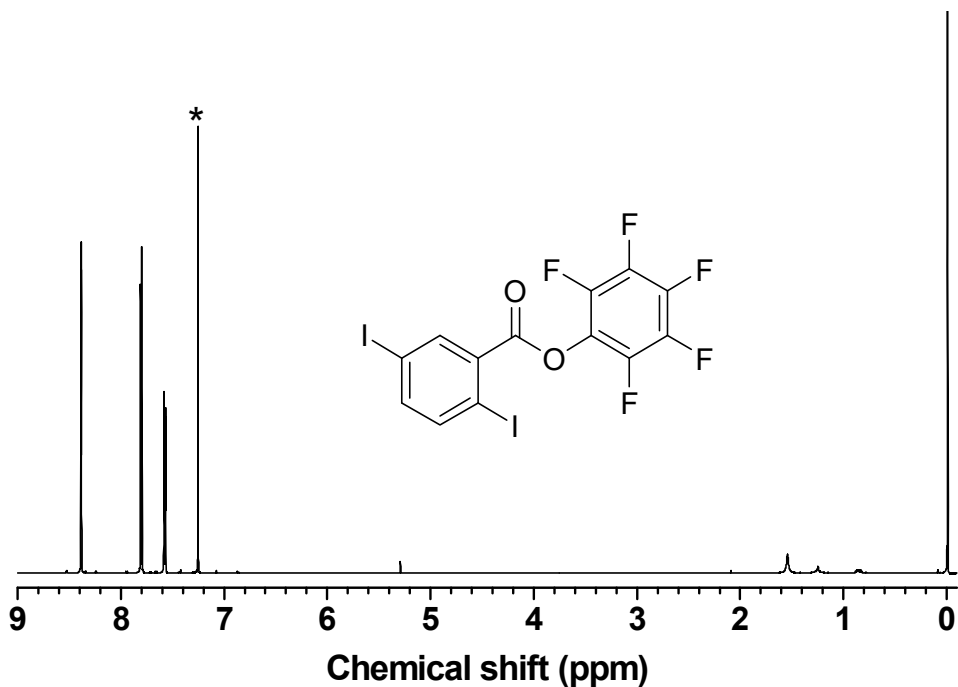


Figure S3. ¹H NMR spectrum of PFDI in CDCl₃. The solvent peak was marked with asterisks.

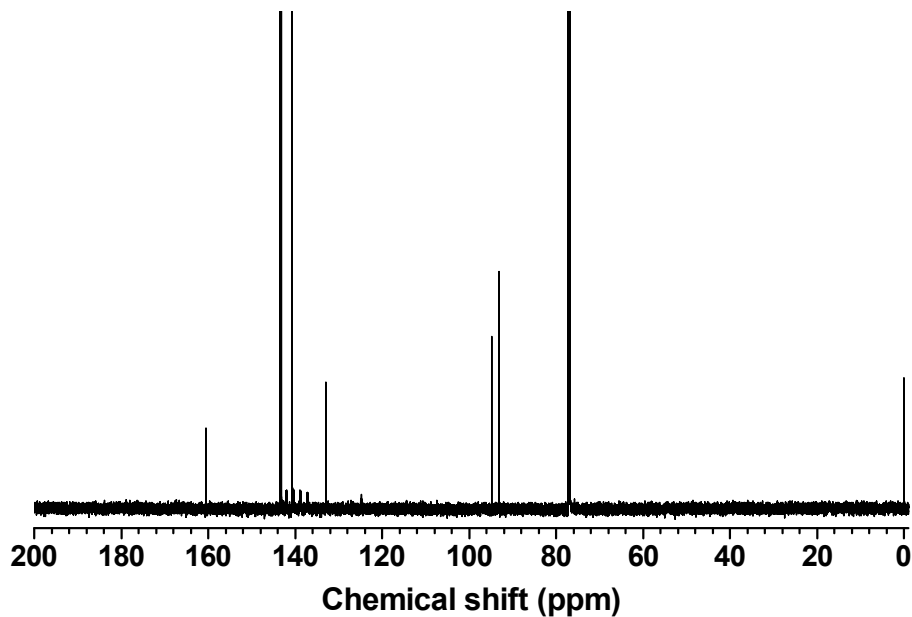


Figure S4. ¹³C NMR spectrum of PFDI in CDCl₃.

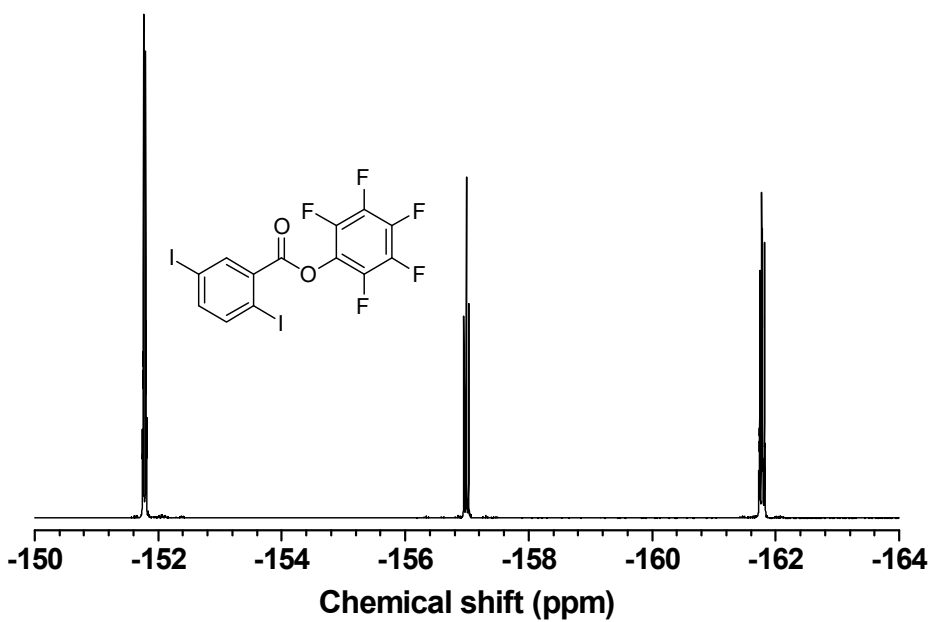


Figure S5. ^{19}F NMR spectrum of **PFDI** in CDCl_3 .

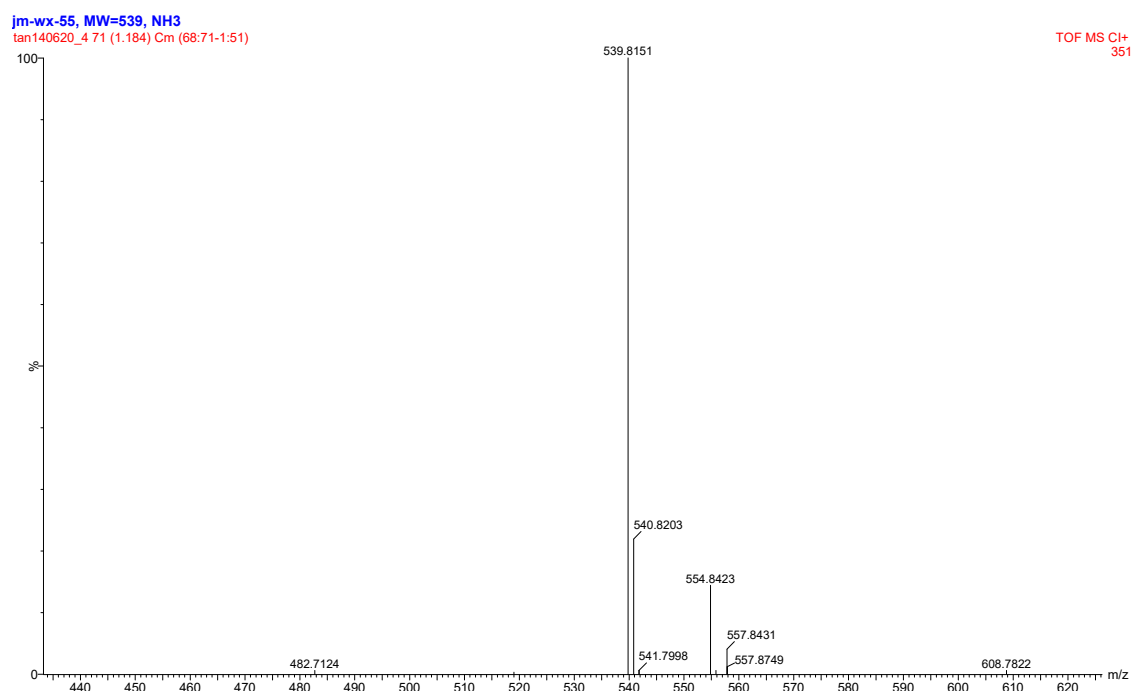


Figure S6. HRMS of the **PFDI**. Calculated: 539.8143. Found: 539.8151

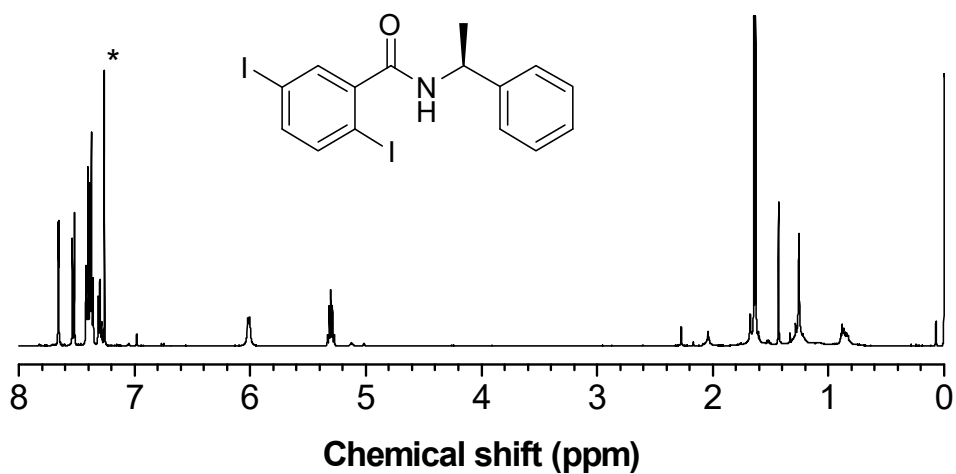


Figure S7. ^1H NMR spectrum of the model compound in CDCl_3 . The solvent peak was marked with asterisks.

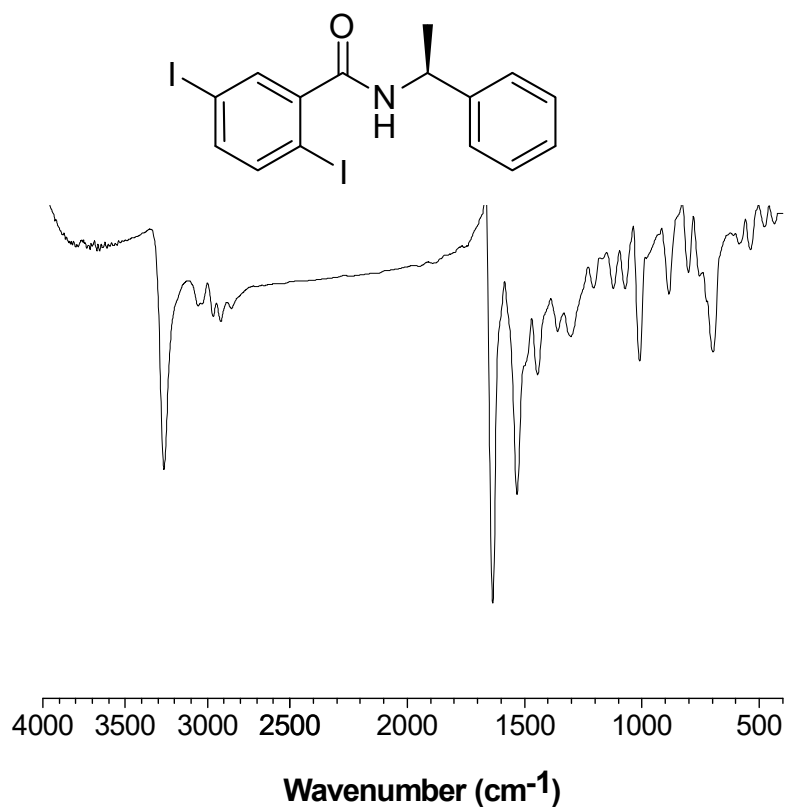


Figure S8. FTIR spectrum of the model compound.

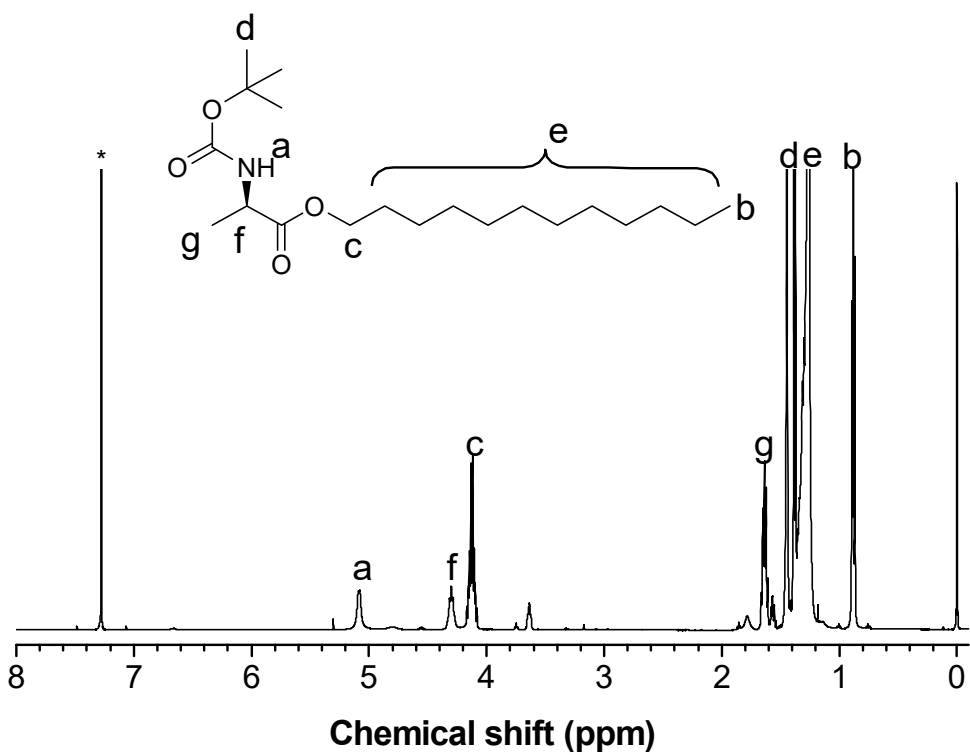


Figure S9. ^1H NMR spectrum of intermediate in CDCl_3 . The solvent peak was marked with asterisks.

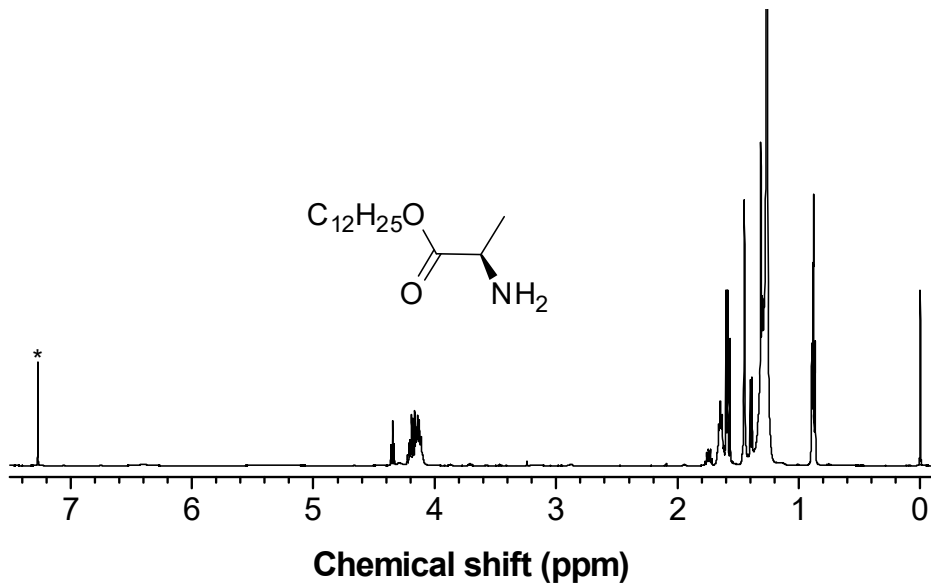


Figure S10. ^1H NMR spectrum of **M1** in CDCl_3 . The solvent peak was marked with asterisks.

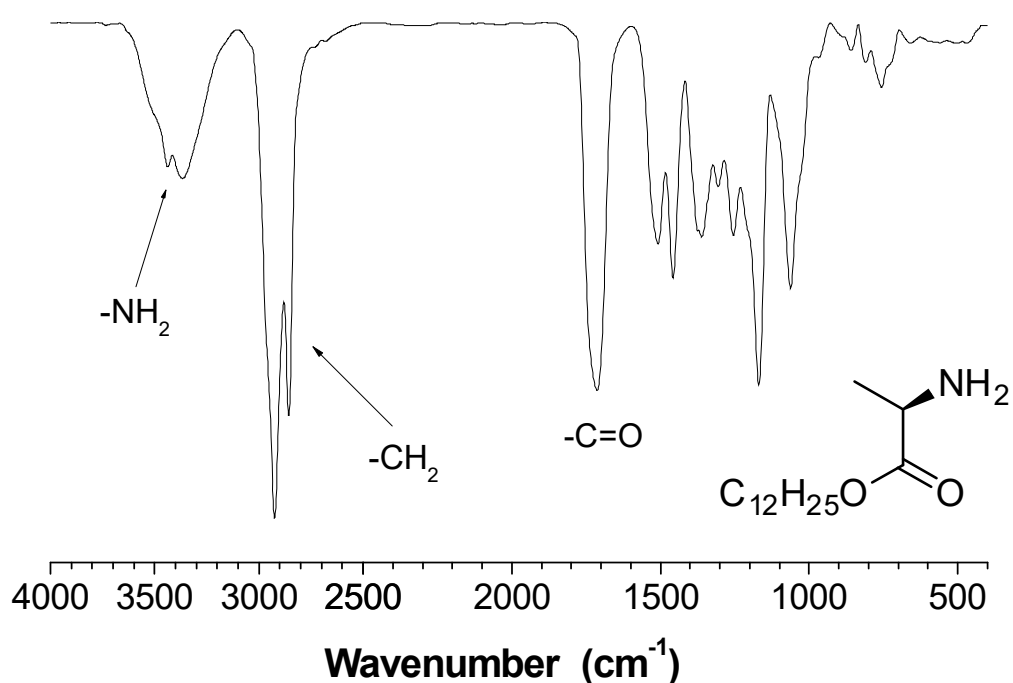


Figure S11. FTIR spectrum of **M1** in thin film.

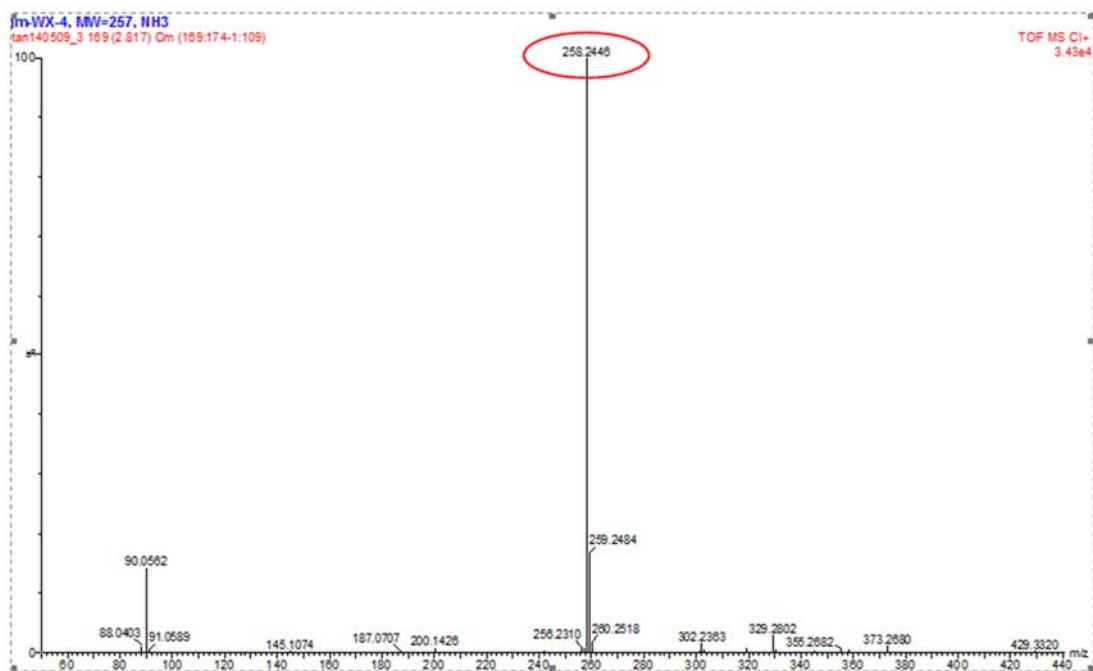


Figure S12. HRMS of **M1**. Calculated: 257.2355. Found: 258.2446.

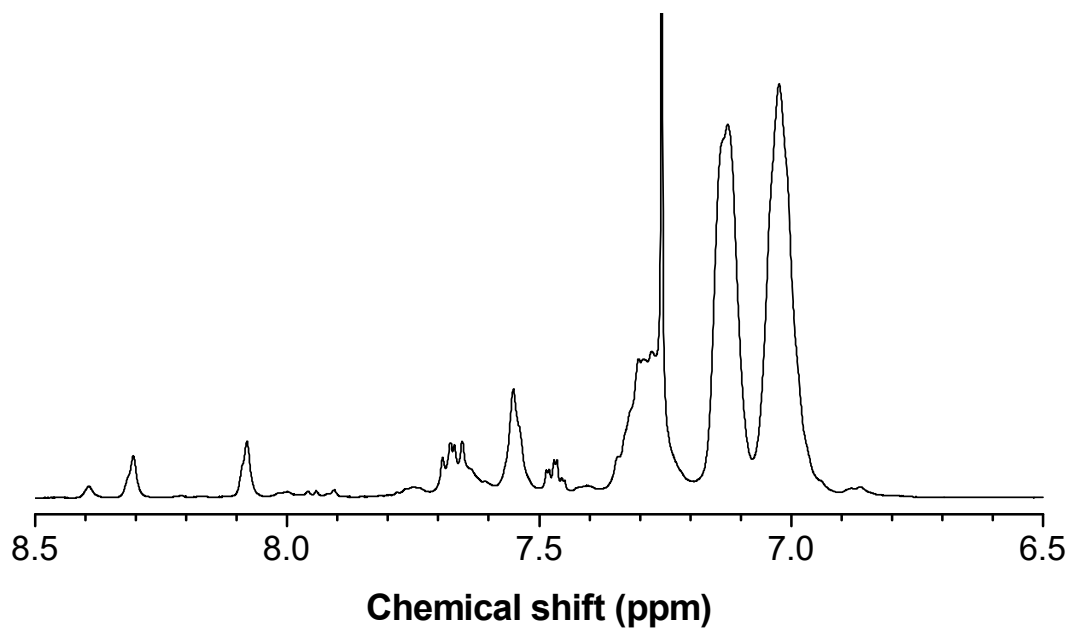


Figure S13. ¹H NMR spectrum of **P0** in CDCl₃.

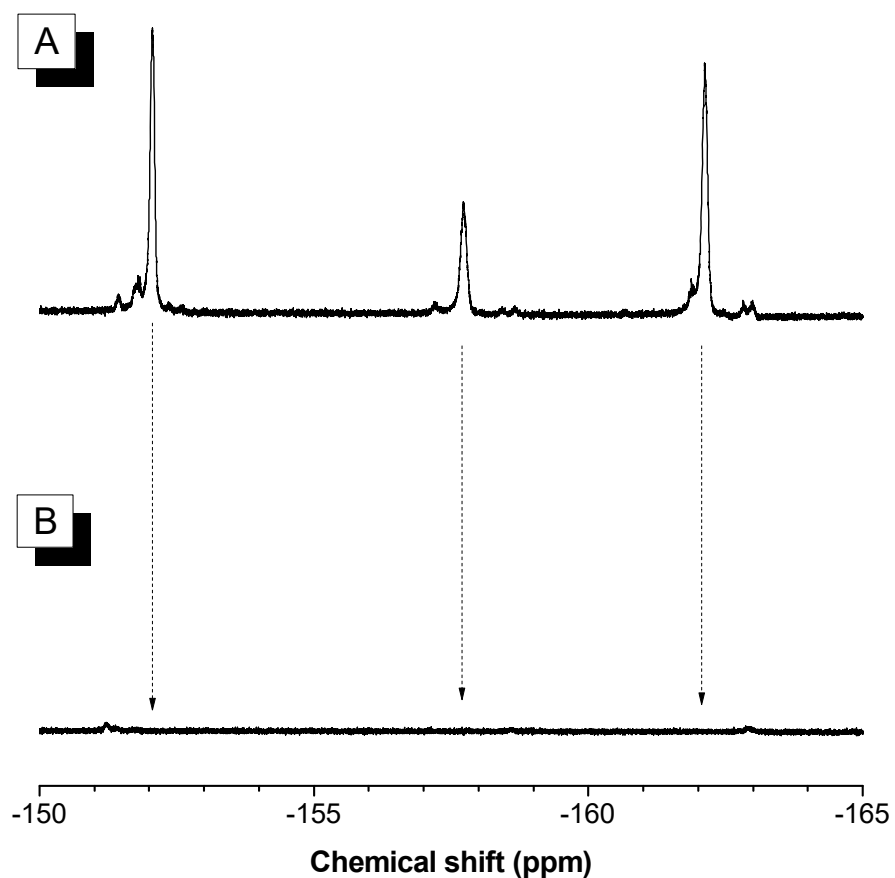


Figure S14. ¹⁹F NMR spectra of (A) **P0** and (B) **P1** in CDCl₃.

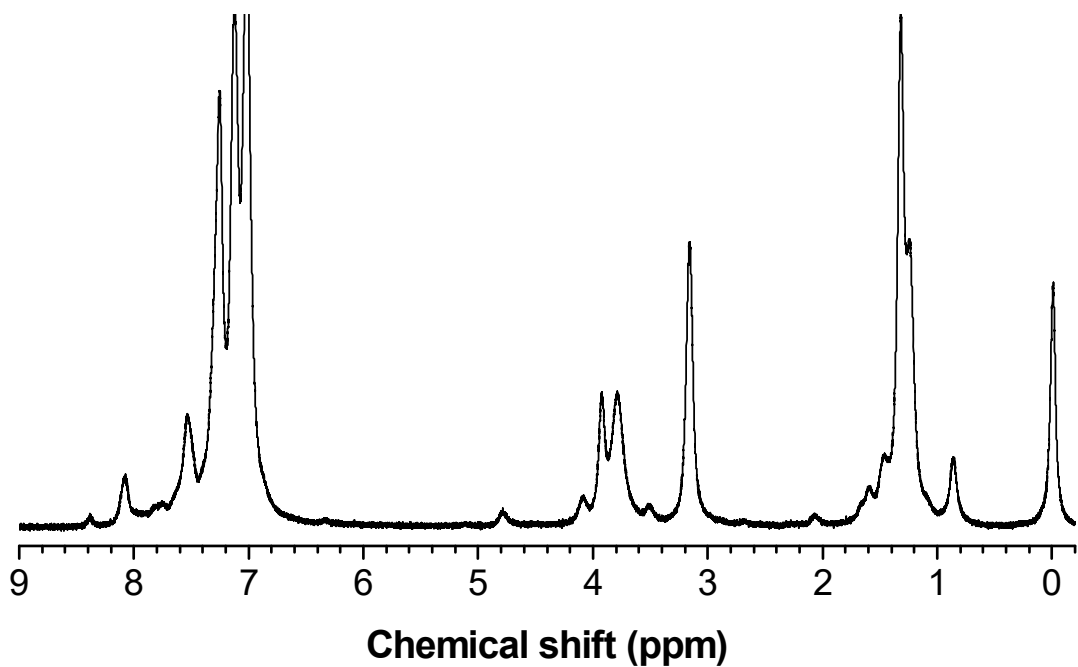


Figure S15. ¹H NMR spectrum of **P1** in CDCl_3 .

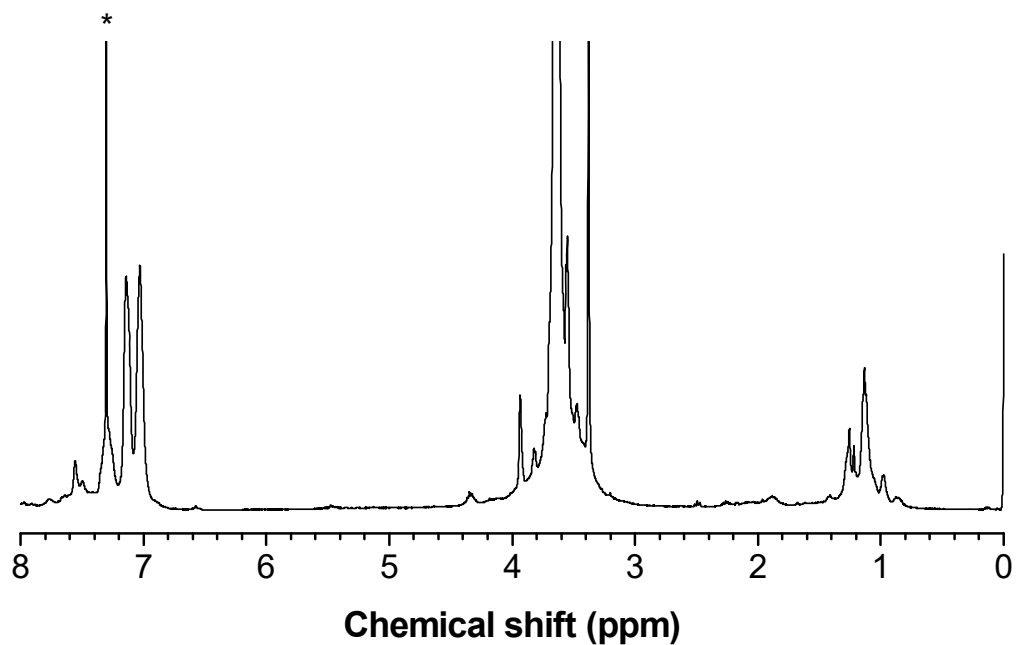


Figure S16. ¹H NMR spectrum of **P2** in CDCl_3 . The solvent peak was marked with asterisks.

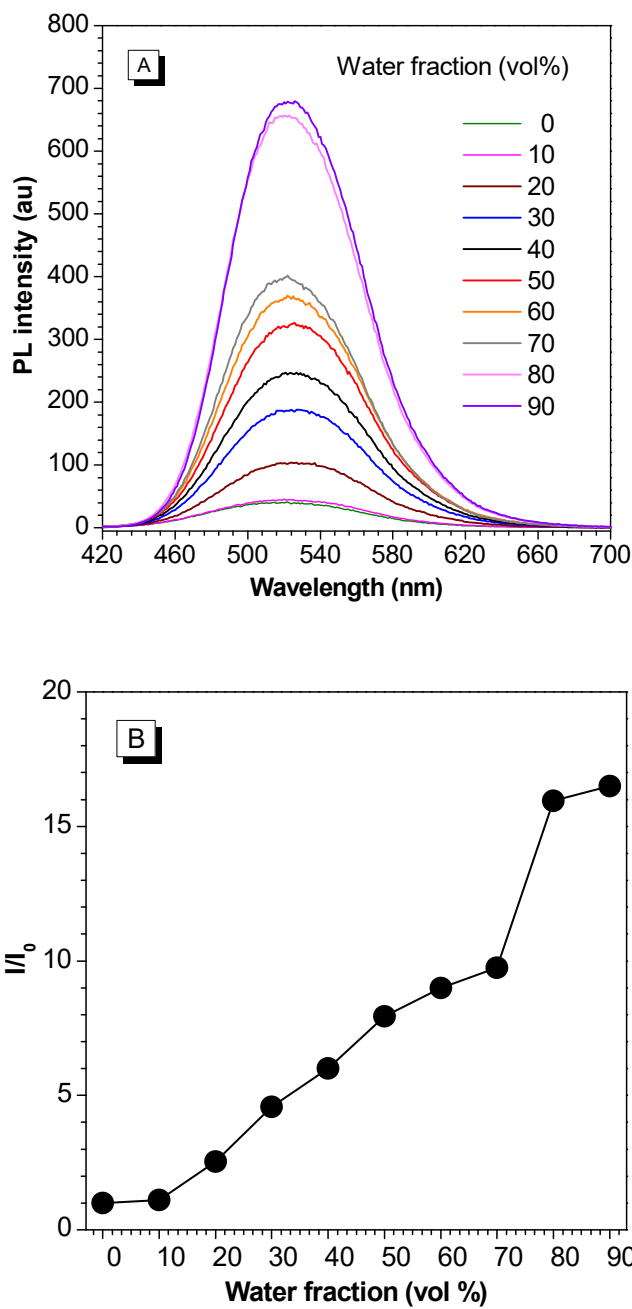


Figure S17. (A) PL spectra of **P1** in THF/water mixtures with different water fractions. Concentration: 10 μ M, $\lambda_{\text{ex}} = 382$ nm. (B) Plot of peak PL intensity of **P1** in THF/water mixtures with different water fractions.

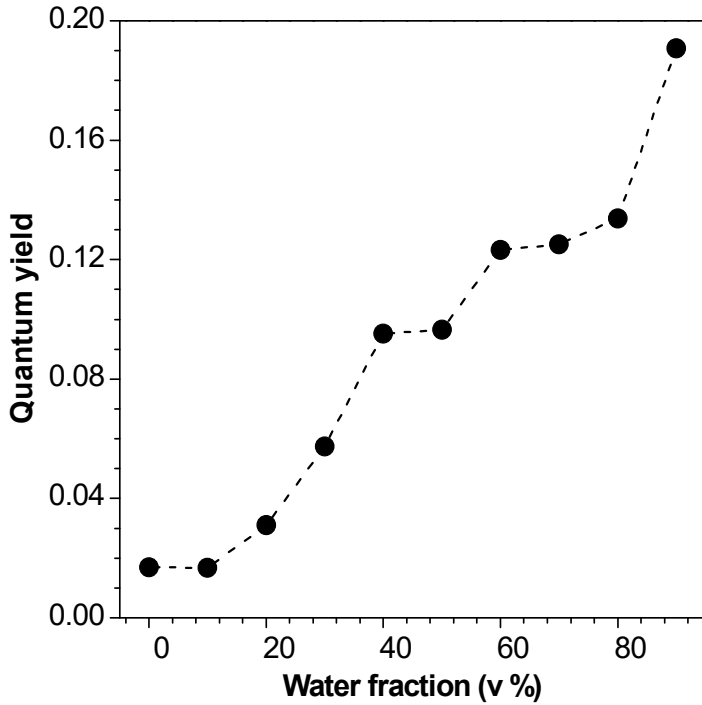


Figure S18. Quantum yield of **P1** in THF/water mixture with different water fractions. **P1** concentration: 10 μM , $\lambda_{\text{ex}} = 382 \text{ nm}$. Aqueous solution of quinine sulfonate ($\Phi = 30\%$) was used as the standard of fluorescence quantum yield.

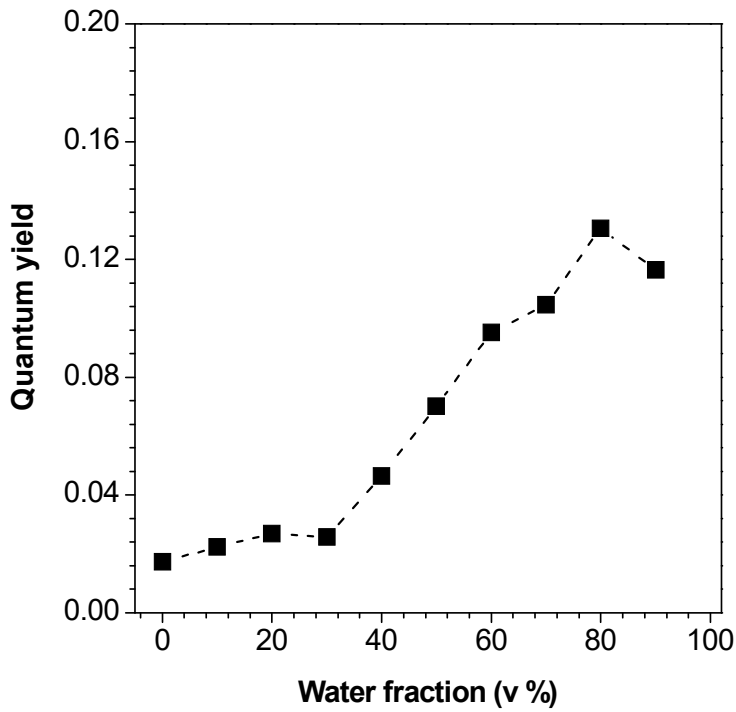


Figure S19. Quantum yield of **P2** in THF/water mixture with different water fractions. **P2** concentration: 10 μM , $\lambda_{\text{ex}} = 377 \text{ nm}$. Aqueous solution of quinine sulfonate ($\Phi = 30\%$) was used as the standard of fluorescence quantum yield.

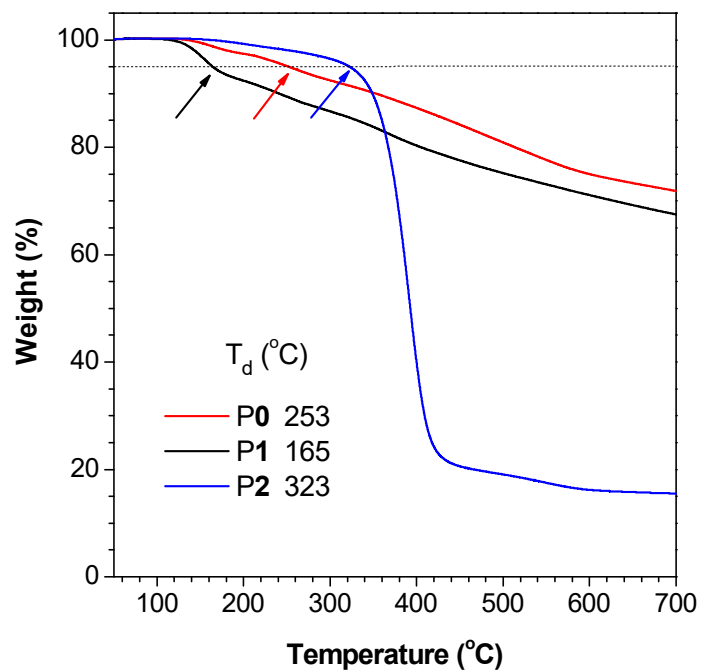


Figure S20. Thermal gravity analysis of P0, P1 and P2 under N_2 atmosphere with a heating rate of 10 $^{\circ}\text{C}/\text{min}$.

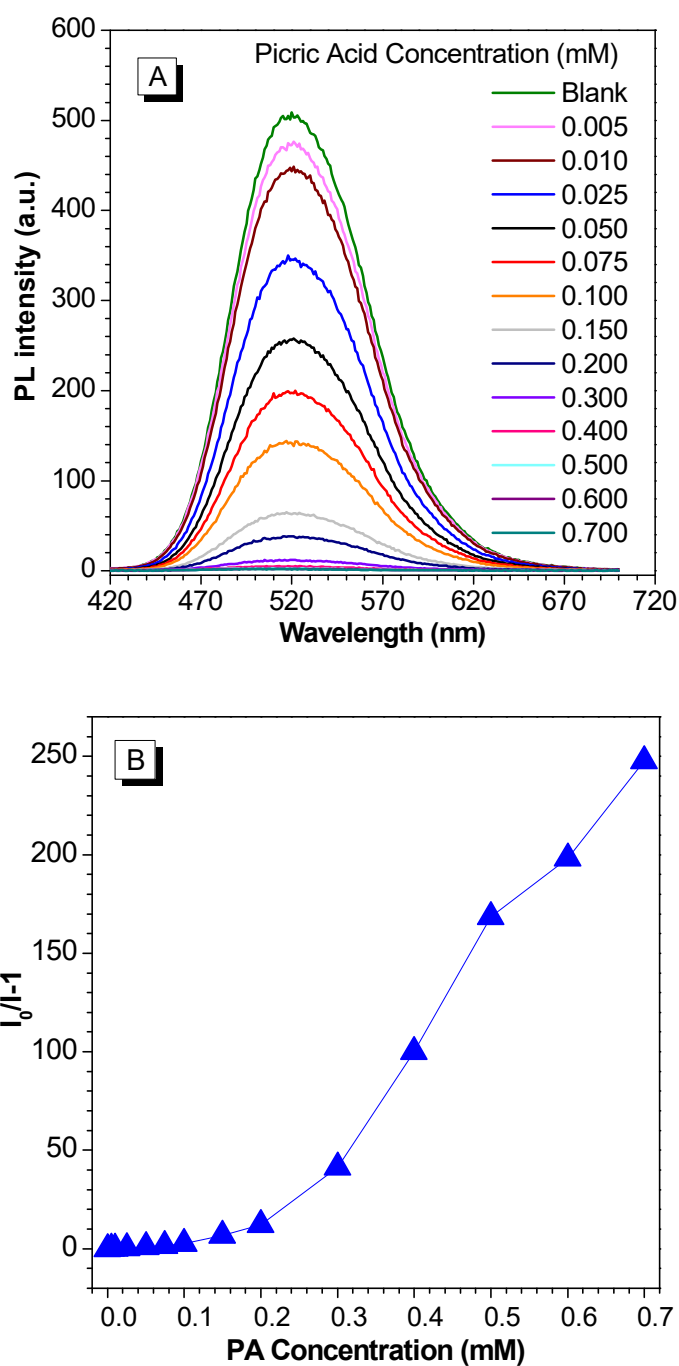


Figure S21. (A) PL spectra of P1 in THF/water mixture (1:9 by volume) with different amount of PA. Polymer concentration: 10 μ M. $\lambda_{\text{ex}} = 382$ nm. (B) Stern-Volmer plot of $I_0/I - 1$ versus [PA] in THF/water mixture with $f_w = 90\%$. I = peak intensity at $[\text{PA}] \neq 0$ mM and I_0 = peak intensity at $[\text{PA}] = 0$ mM.

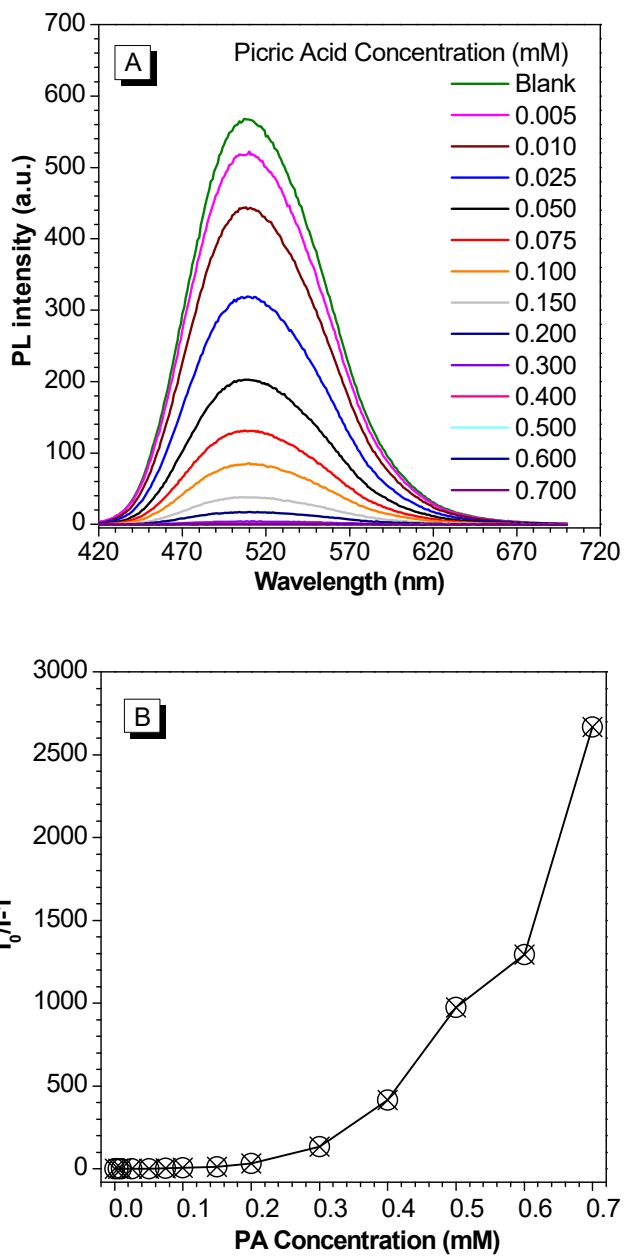


Figure S22. (A) PL spectra of **P2** in THF/water mixtures (1:9 by volume) with different amount of PA. Polymer concentration: 10 μ M. Excitation wavelength: 377 nm. (B) Stern-Volmer plots of $I_0/I - 1$ versus [PA] in THF/water mixtures with $f_w = 90\%$. I = peak PL intensity at $[PA] \neq 0$ mM, and I_0 = peak PL intensity at $[PA] = 0$ mM.